Electronic supporting information

High performance hydrogen photoproduction using Co-doped CuBDC metal organic framework

Sher Mohd,[a] Lavinia Balan,[b] Thomas Gries,[c] Halima Alem,[c] Ghouti Medjahdi,[c] Maud Lebrun,[a] Véronique Falk,[a] Raphaël Schneider [a*]

[a] Université de Lorraine, CNRS, LRGP, F-54000 Nancy, France

[b] CNRS, Université d'Orléans, CEMTHI, 1 Av. de la Recherche Scientifique, Orléans, France

[c] Université de Lorraine, CNRS, IJL, F-54000 Nancy, France

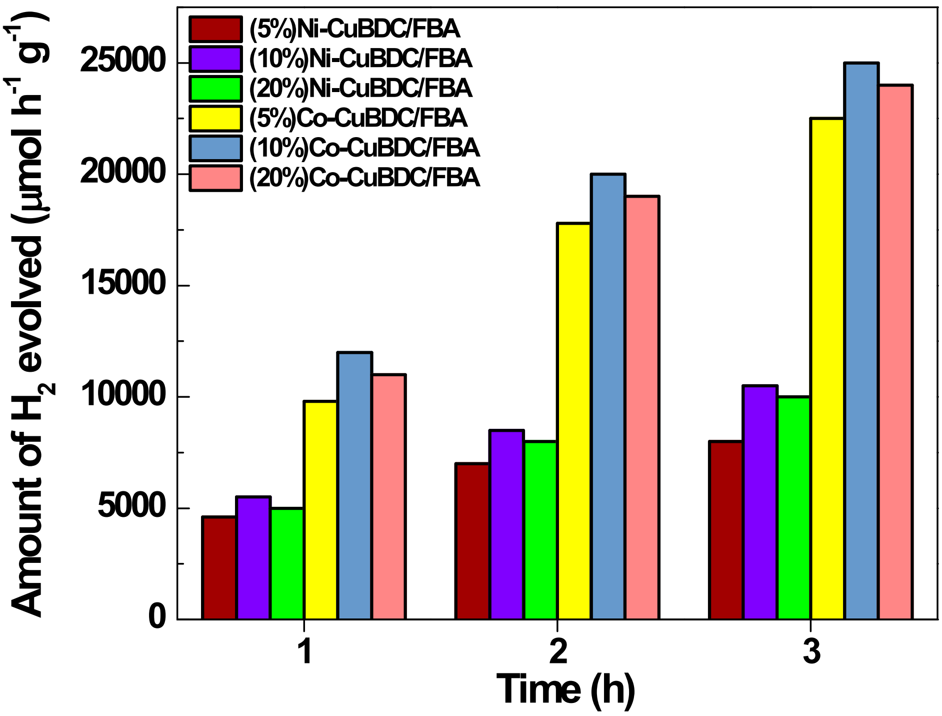

Fig. S1. Photocatalytic H_2 evolution for Ni-CuBDC and Co-CuBDC when varying the Ni or Co dopant percentage.

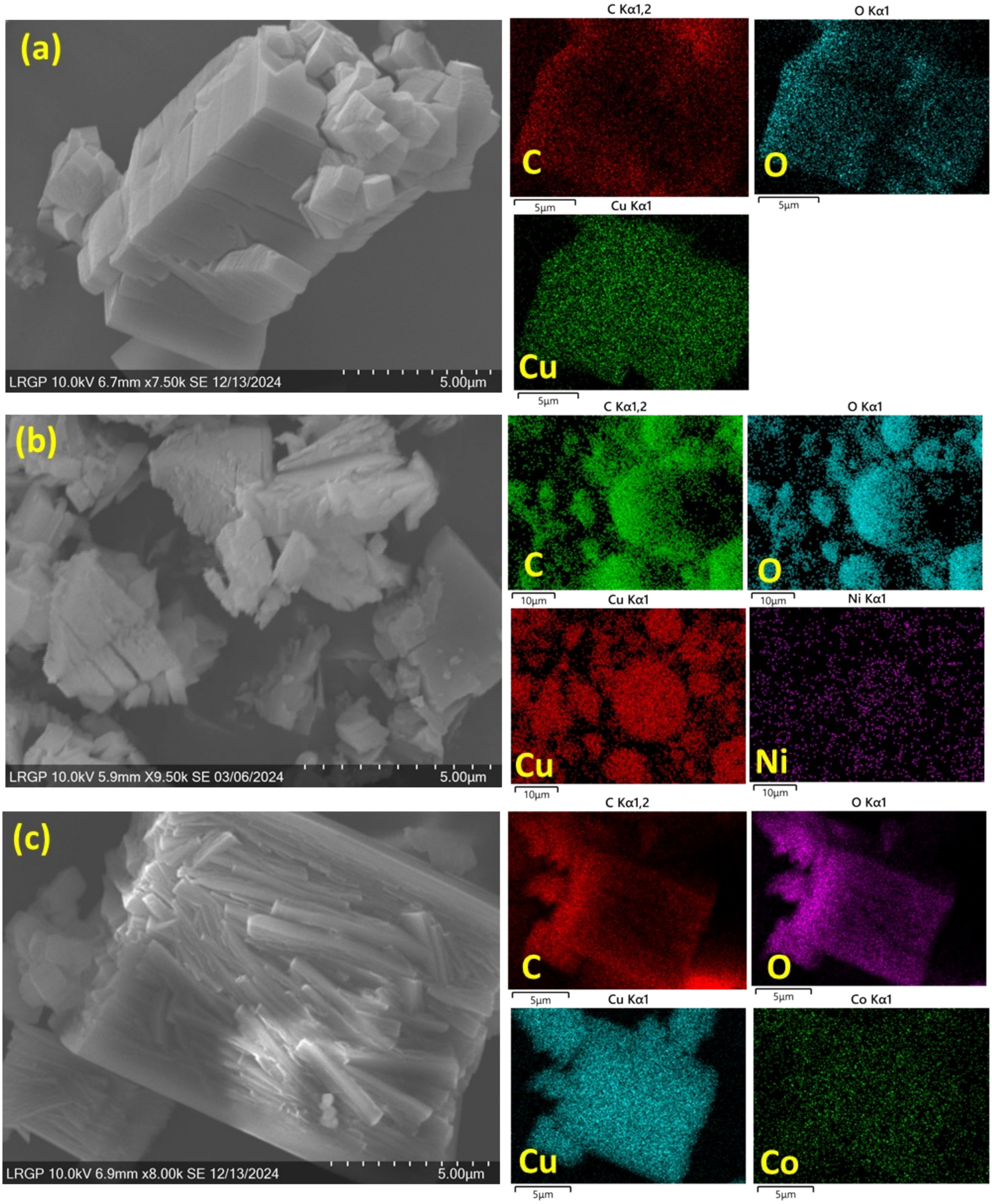

Fig. S2. SEM images of (a) CuBDC, (b) Ni-CuBDC and (c) Co-CuBDC and the corresponding elemental mapping.

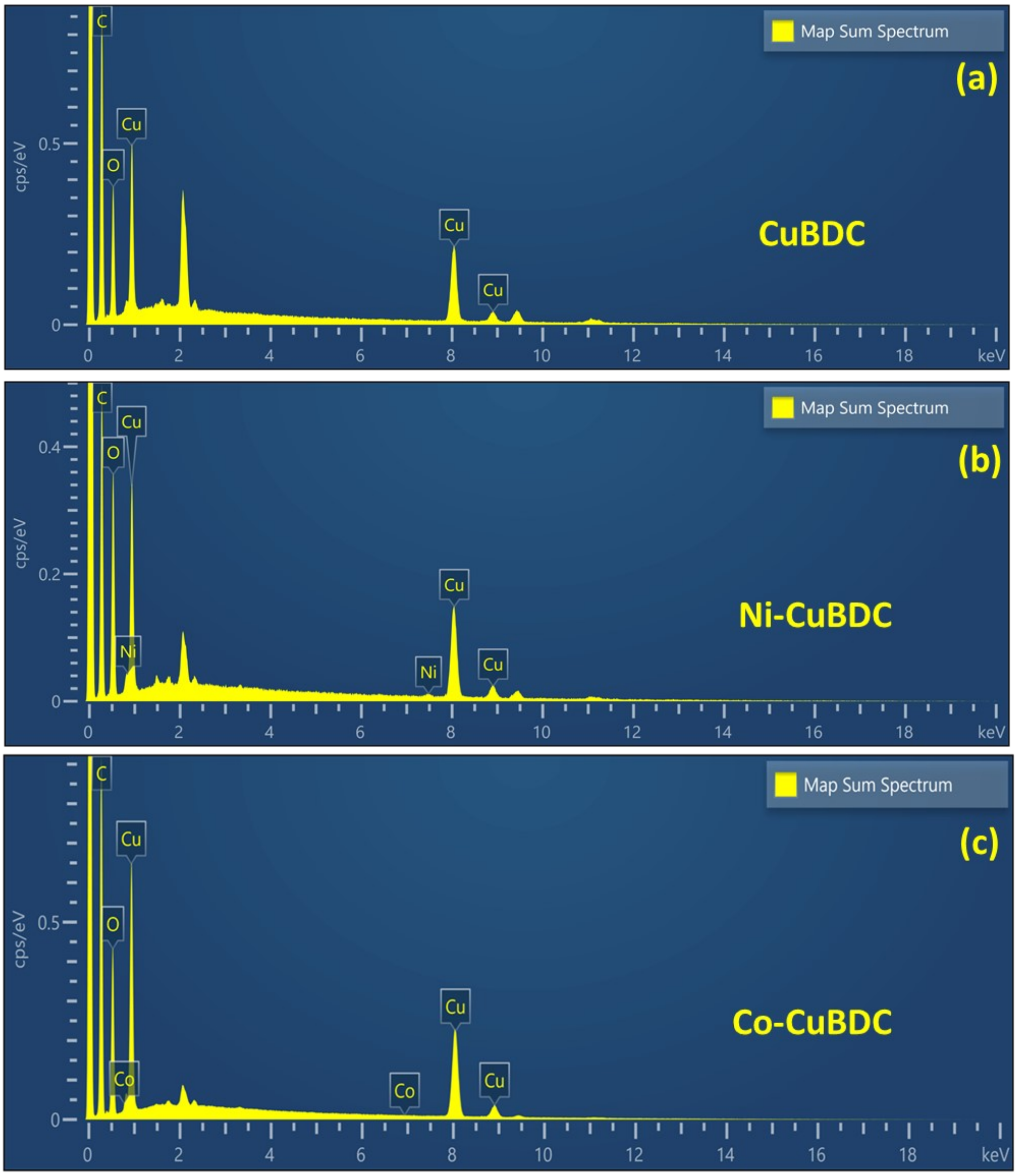

Fig. S3. EDX analyses of (a) CuBDC, (b) Ni-CuBDC and (c) Co-CuBDC.

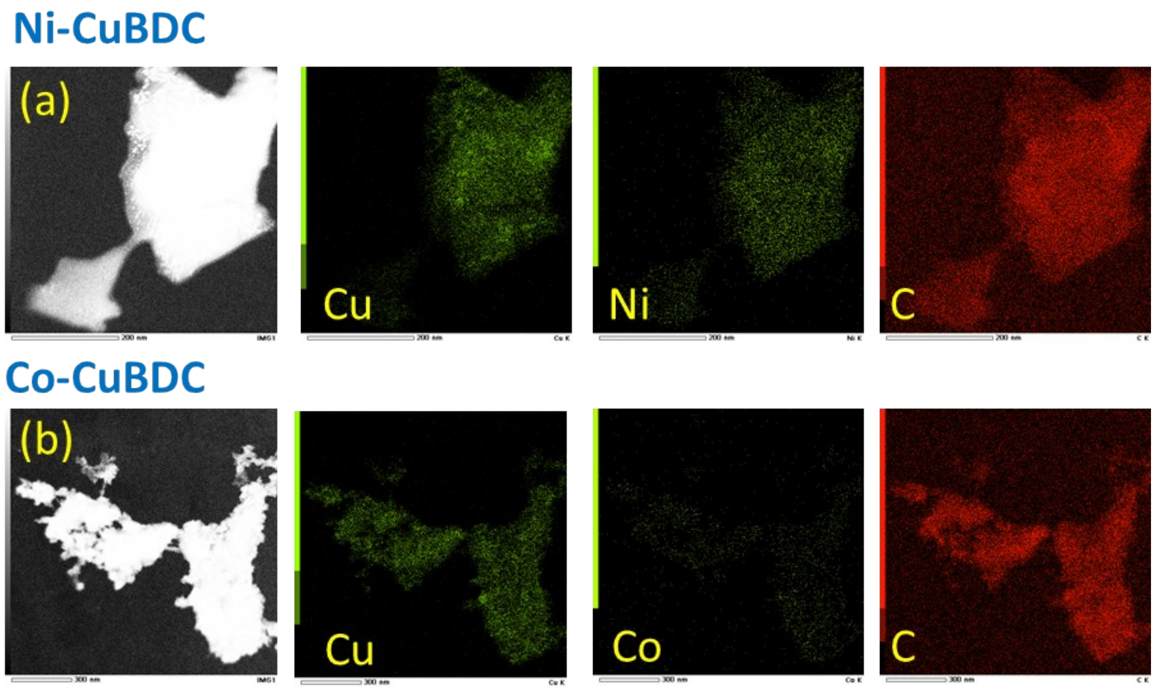

Fig. S4. TEM images of (a) Ni-CuBDC and (b) Co-CuBDC and the associated elemental mappings.

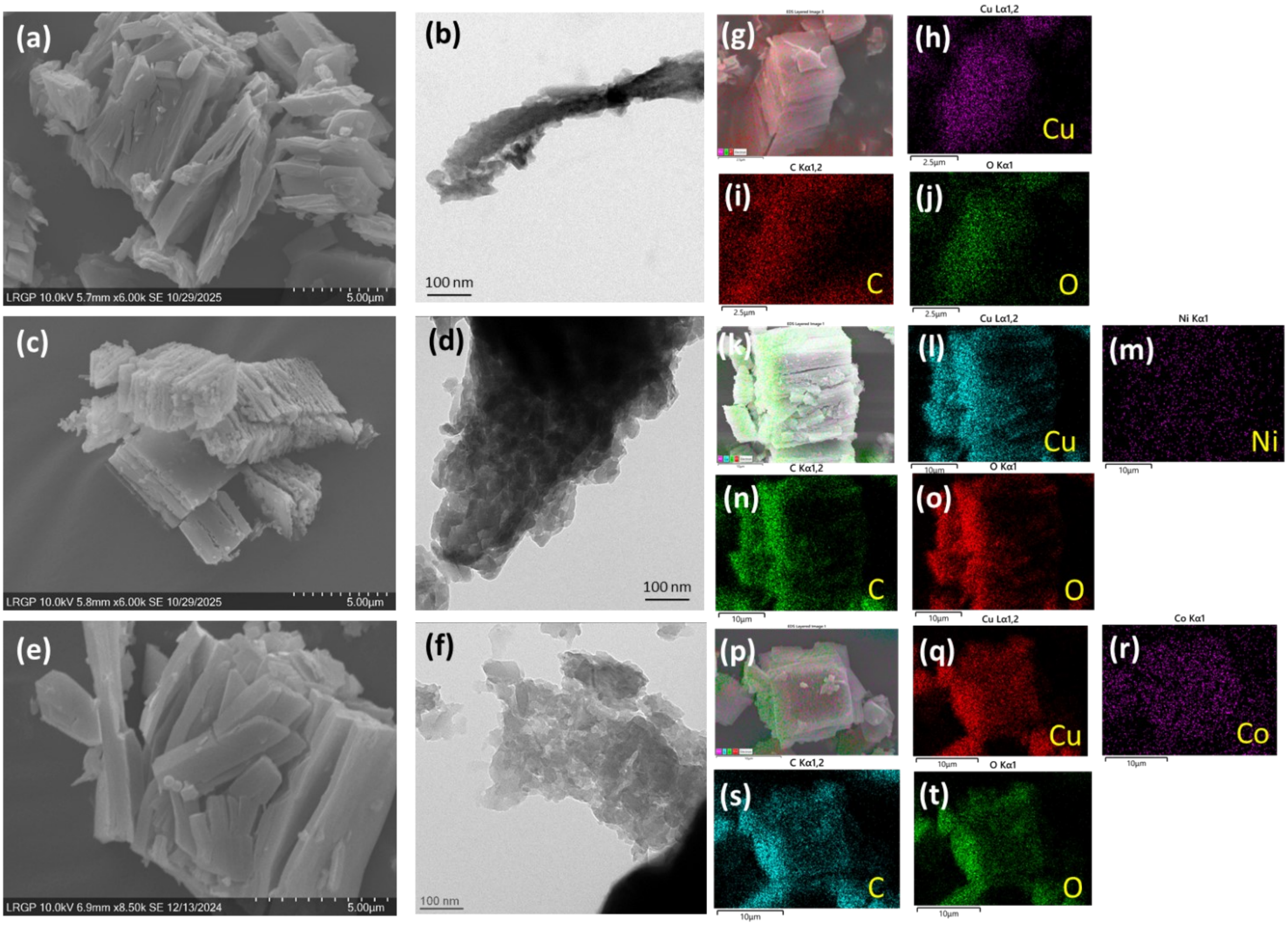

Fig. S5. (a,c,e) TEM (b,d,f) SEM images of CuBDC, Ni-CuBDC and Co-CuBDC prepared in the absence of 4-FBA, respectively. (g-t) the corresponding SEM-associated EDX elemental mappings.

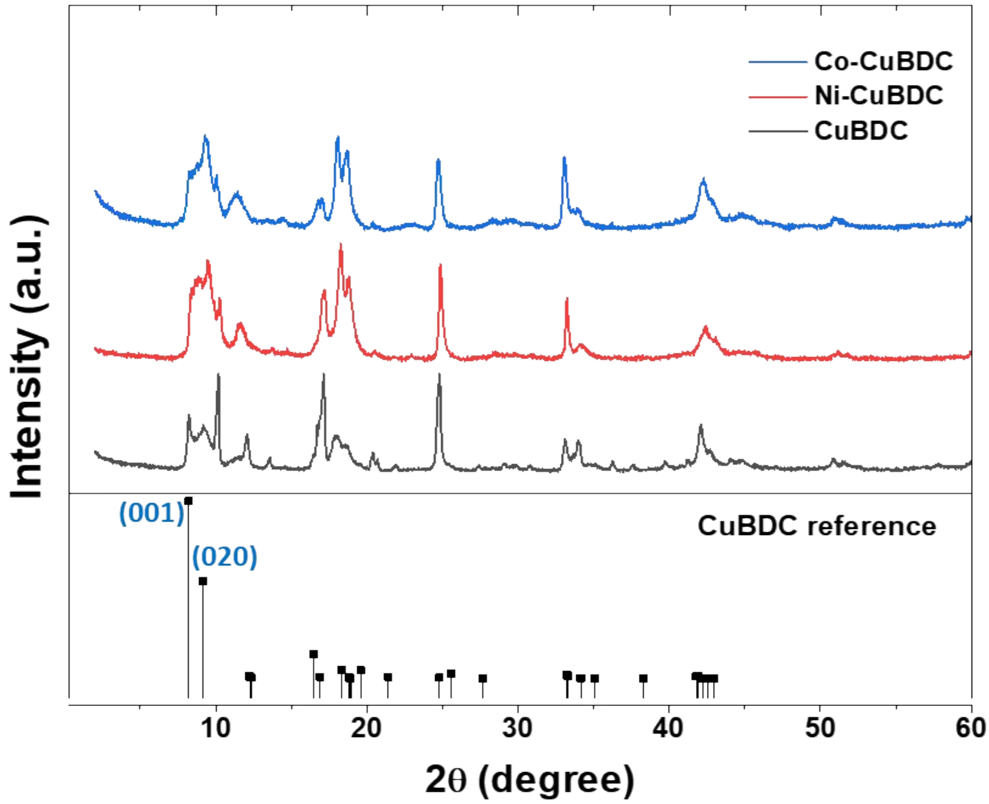

Fig. S6. XRD patterns of CuBDC, Ni-CuBDC, Co-CuBDC and of the CuBDC reference.

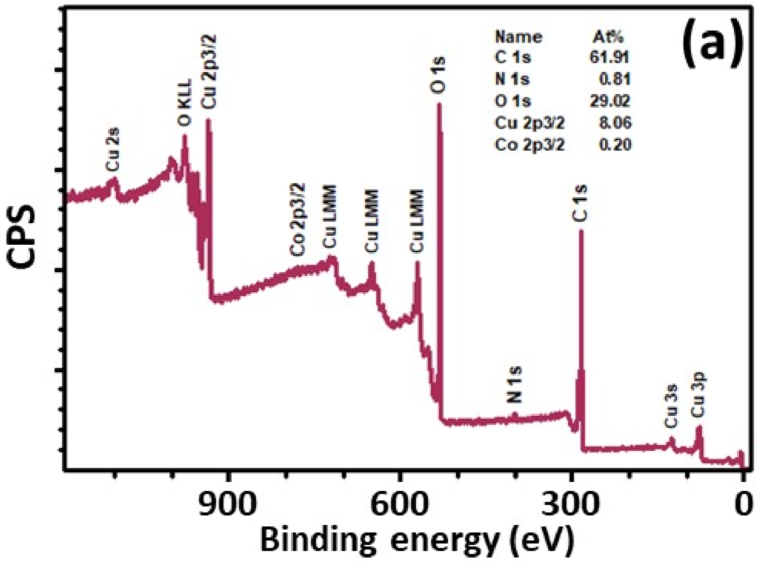

Fig. S7. Overview XPS spectrum of Co-CuBDC.

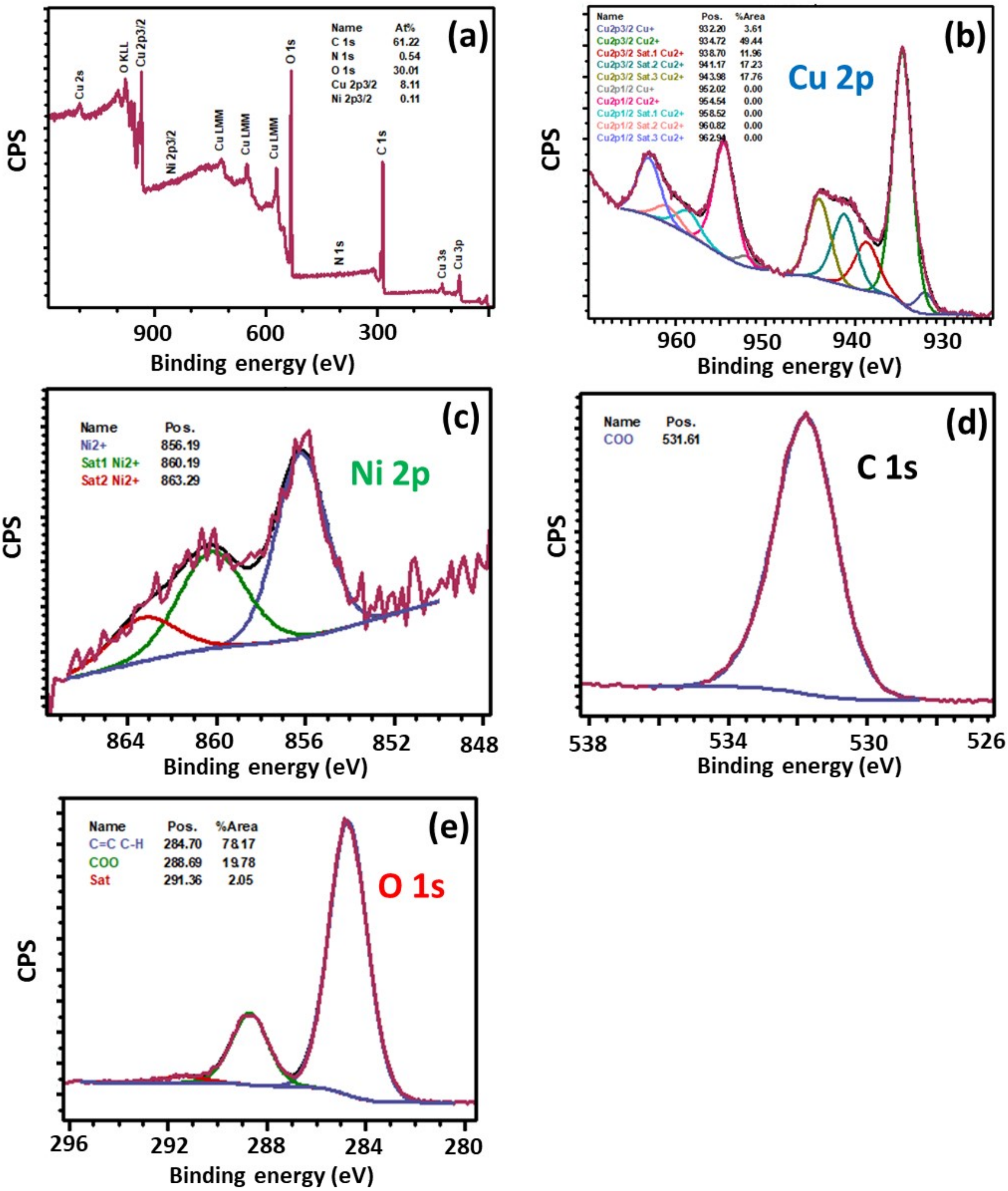

Fig. S8. (a) Overview XPS spectrum of Ni-CuBDC and high resolution XPS spectra of (b) Cu 2p, (c) Ni 2p, (d) C 1s and (e) O 1s.

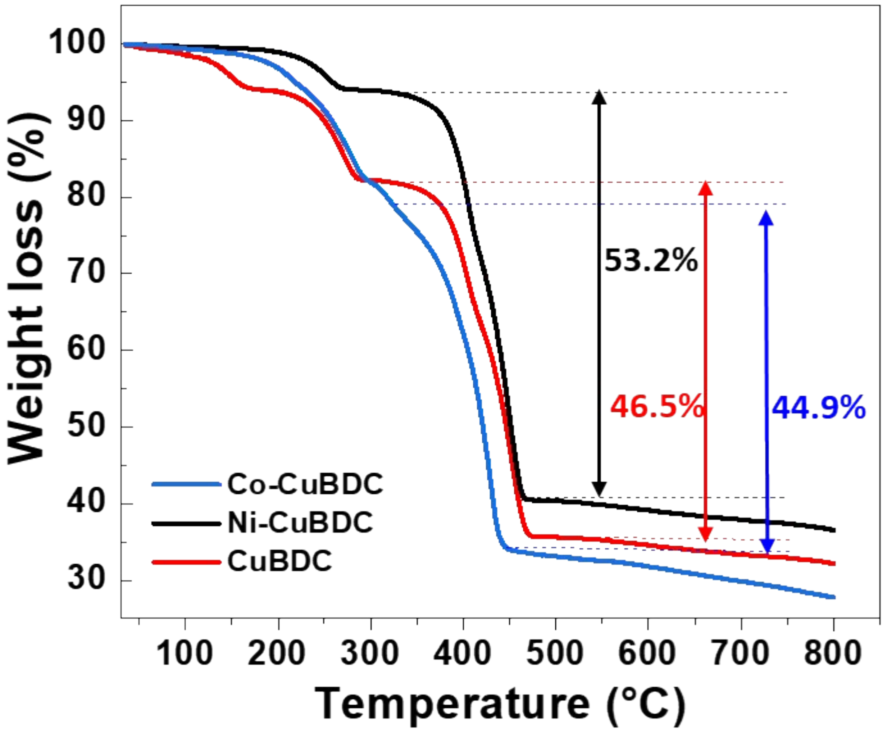

Fig. S9. TGA profiles of CuBDC, Ni-CuBDC and Co-CuBDC from 40 to 800°C.

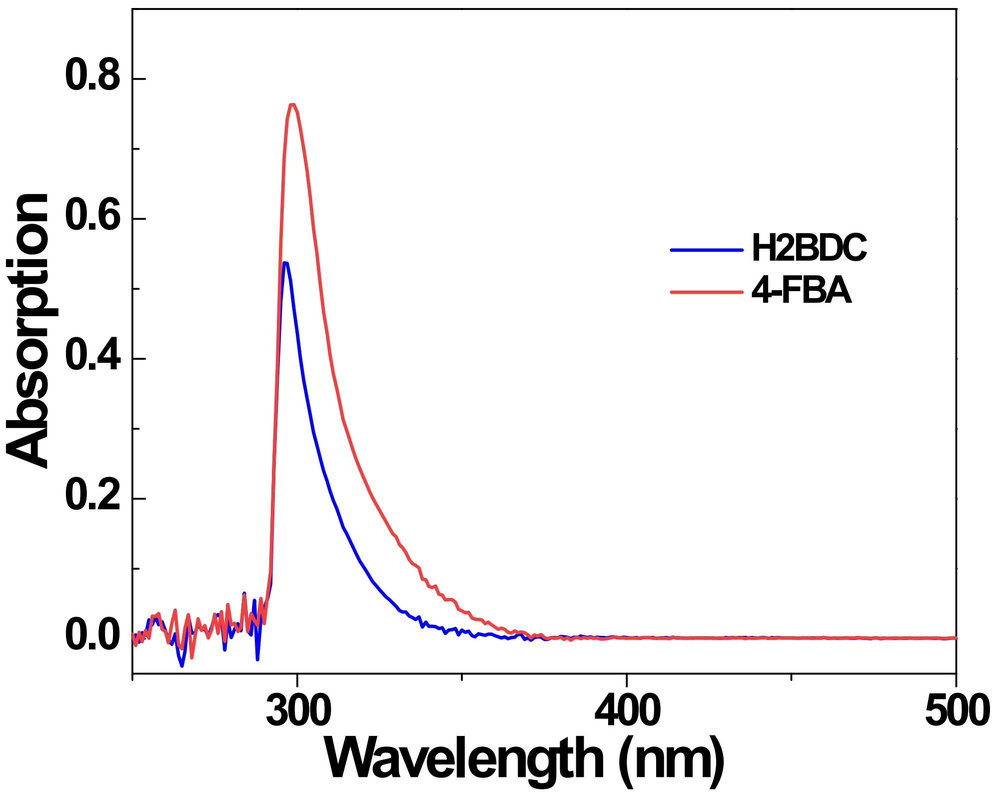

Fig. S9. UV-visible absorption spectra of H2BDC and 4-FBA in DMF.

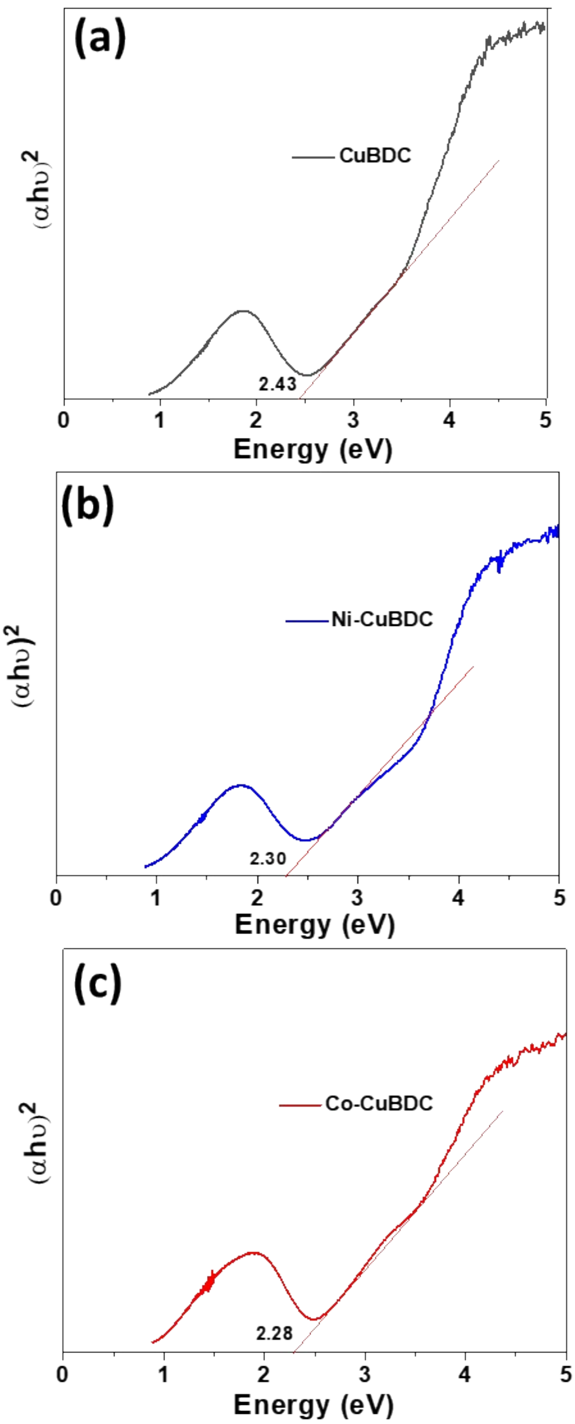

Fig. S10. Tauc plots of (a) CuBDC, (b) Ni-CuBDC and (c) Co-CuBDC.

Table S1. Impedance parameters obtained after fitting the EIS curves with the simplified Randles equivalent circuit comprising a solution resistance (Rs), a charge transfer resistance (Rct) and a constant phase element (CPE) to account for the non-ideal double-layer capacitance.

Sample	Rs (Ω)	Q ($F.s^{\alpha-1}$)	α	Rct (Ω)
Ni-CuBDC	44,8	$3{,}054.10^{-5}$	0,8149	747,5
Co-CuBDC	63,1	$2{,}452.10^{-4}$	0,8781	660,8
CuBDC	16,5	$4{,}876.10^{-4}$	0,7857	1564

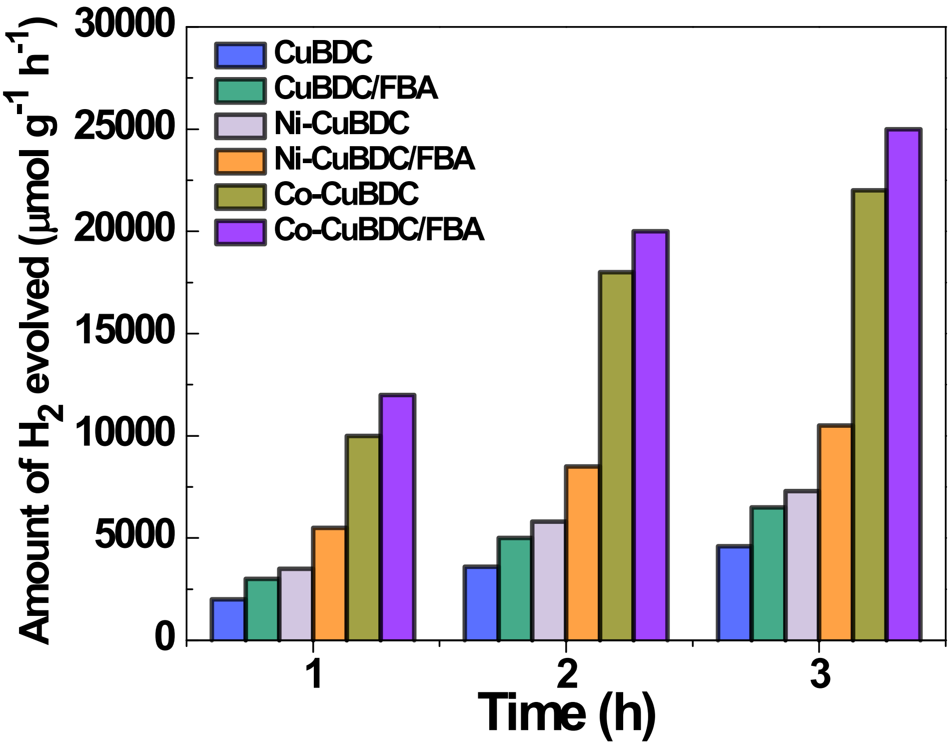

Fig. S11. Photocatalytic H_2 evolution for CuBDC, Ni-CuBDC and Co-CuBDC prepared in the absence or presence of the FBA defective linker.

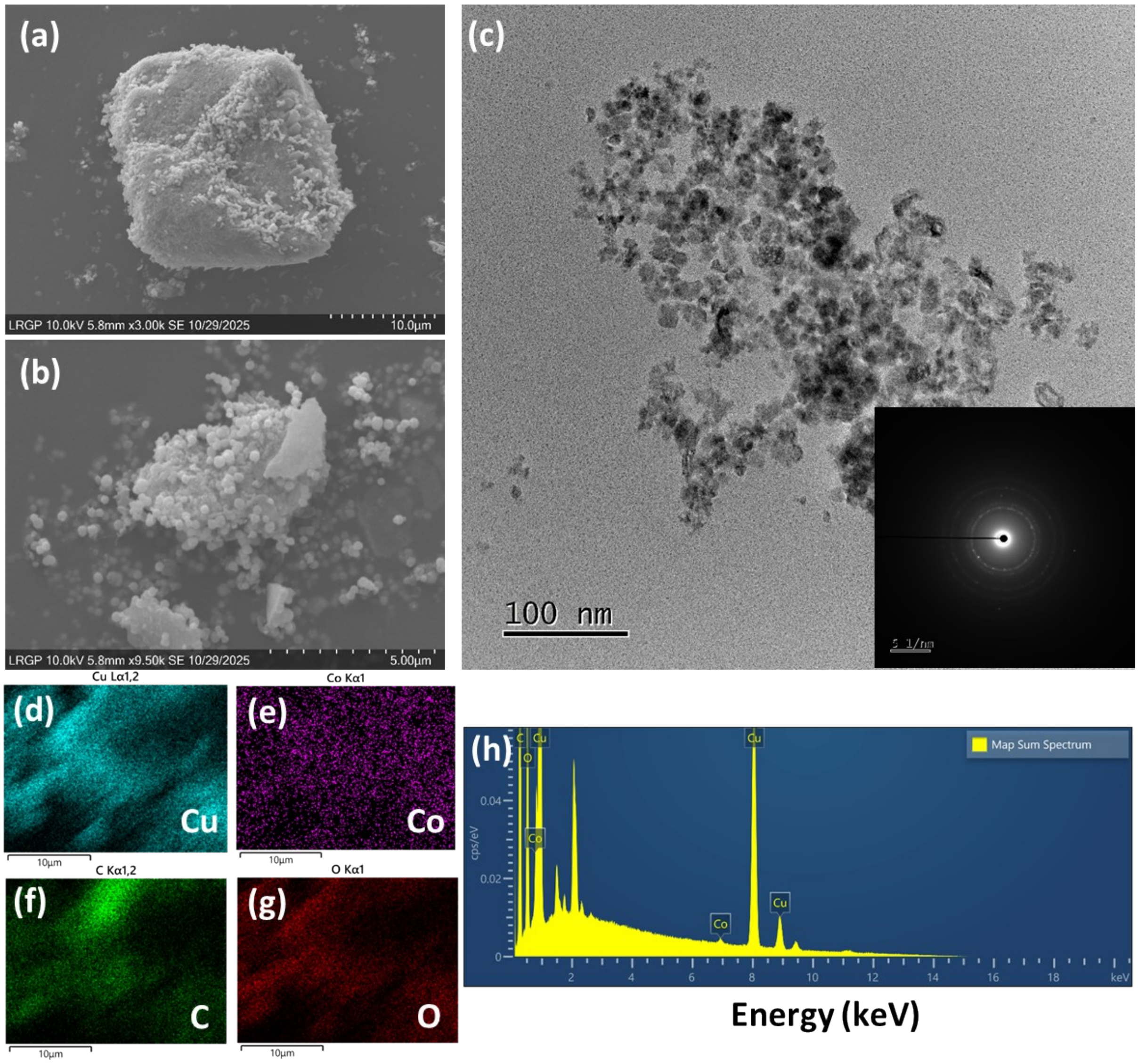

Fig. S12. (a,b) SEM and (c) TEM images of the Co-CuBDC photocatalyst after 3 cycles of H_2 production, (d-h) the SEM-associated EDX elemental mapping and (i) EDX analysis. The inset of (c) is the SAED pattern.

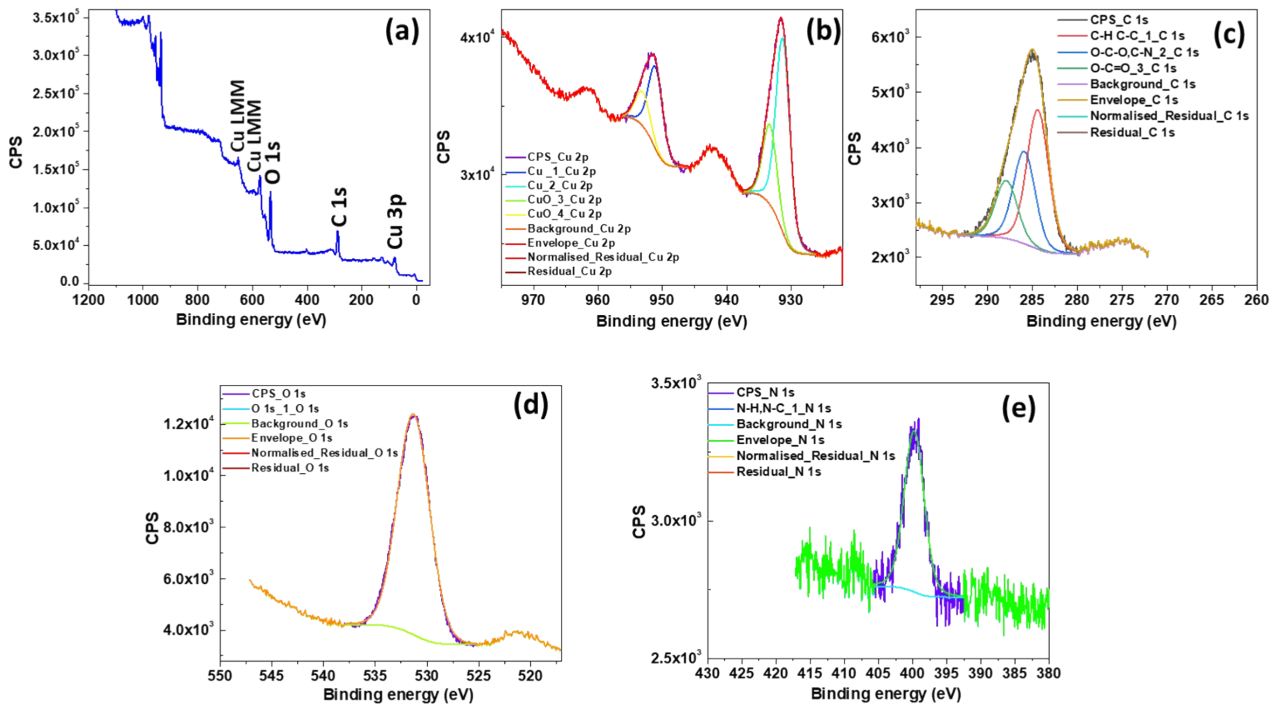

Fig. S13. (a) Overview XPS spectrum of the reused Co-CuBDC photocatalyst and HR XPS spectra of (b) Cu 2p, (c) C 1s, (d) O 1s and (e) N1s.

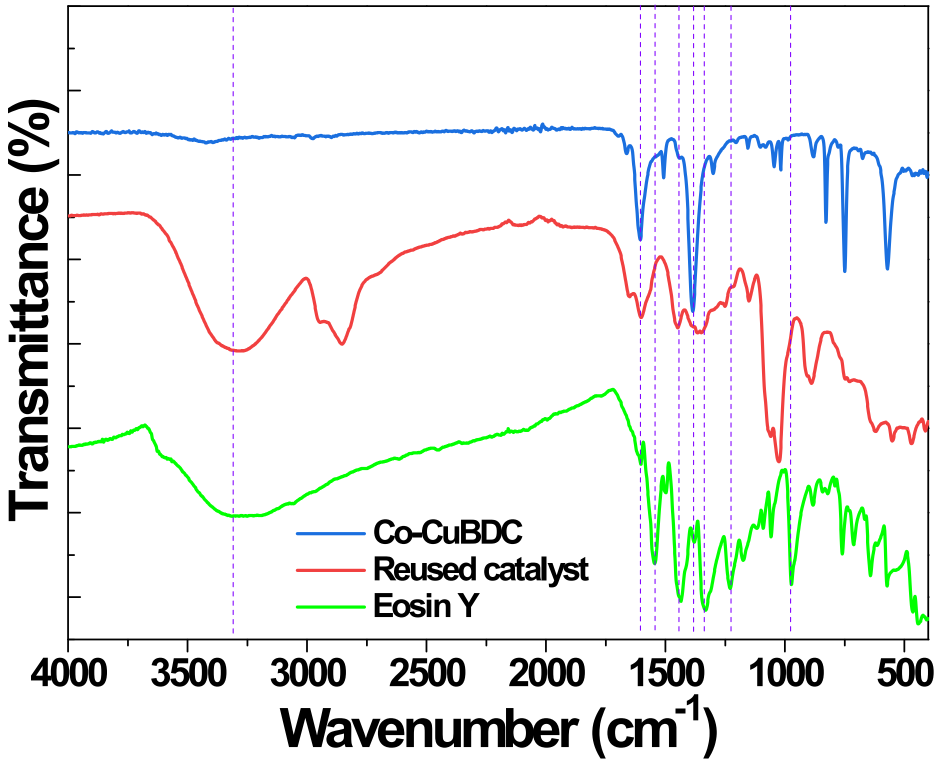

Fig. S14. FT-IR spectra of Eosin Y, Co-CuBDC and of the reused Co-CuBDC photocatalyst.

Table S2. Comparison of the performance of of MOF-based photocatalysts for H_2 production.

Catalyst	**Operating conditions**	**H_2 evolved**	**Reference**
UiO-66/Pd (3 wt%)	10 mg catalyst in 30 mL of 15% aqueous TEOA, 20 mg EY, 5 W LED (420 nm)	2357 µmol.h^{-1}.g^{-1}	1
UiO-66-NH_2/Ag-Pd	20 mg catalyst in 10% MeOH aqueous solution, 300 W Xe lamp	448.2 µmol h^{-1}	2
UiO-66-NH_2/$ZnIn_2S_4$/Pt	10 mg catalyst in 30 ML acetonitrile containing 33 µL of benzylamine, 300 W Xe lamp with AM 1.5 filter,	5275 µmol.h^{-1}.g^{-1}	3
UiO-66-NH_2/Fe_3O_4	20 mg catalyst in 20 mL MeOH/water (10% v/v), 300 W Xe lamp	417 µmol h^{-1}	4
UiO-66-NH_2/Pt/UiO-66	10 mg catalyst in 18 mL acetonitrile, 1 mL triethylamine (TEA) and 0.5 mL Water, 300 W Xe lamp with UV filter.	2708 µmol.h^{-1}.g^{-1}	5
UiO-66-NH_2/CdS	20 mg catalyst in 80 mL benzyl alcohol aqueous solution, 300 Xe lamp	630 µmol h^{-1} g^{-1}	6
NH_2-MIL-125(Ti) doped with Ni	10 mg catalyst in 4.5 mL of water and 0.5 mL TEOA, 300 W Xe lamp with UV filter	699 µmol h^{-1} g^{-1}	7
NiBDC/CdS	10 mg of catalyst in 30 mL of acetonitrile containing 33 µL of benzylamine and 500 µL of water, 300 W Xe lamp	8500 µmol h^{-1} g^{-1}	8
MIL-127/MIL-125-NH_2	17 mg catalyst in in 17.0 ml of acetonitrile, water and TEA (13.4 mL CH_3CN, 0.8 mL H_2O and 2.8 mL TEA), 300 W Xe lamp with UV filter	455 µmol h^{-1} g^{-1}	9
MIL-53(Sr)/MIL-53(Fe)/Pt	50 mg catalyst in 100 mL water/MeOH (80/20), 300 W Xe lamp	226 µmol h^{-1} g^{-1}	10
Cu-MOF containing fluorinated linker/Pt (0.15 wt%)	80 mg catalyst, water containing 15% EtOH, Rhodamine B, 500 W Xe lamp	63640 µmol h^{-1} g^{-1}	11
CuBTC/CdZnS	10 mg catalyst in 50 mL Na_2SO_3/Na_2S aqueous solution, 300 W Xe lamp with UV filter	18986 µmol h^{-1} g^{-1}	12
CuBTC on Ni foam	5 mg catalyst in 50 mL buffer containg 10% TEOA, EY, 300 W	8000 µmol h^{-1} g^{-1} 24400 µmol h^{-1} g^{-1}	13

	Xe lamp with UV filter.	when using Pt	
CuBDC-NH_2/$Cu_{58}S_{32}$	40 mg catalyst in aqueous Na_2SO_3/Na_2S solution150 W Xe lamp with UV filter	9343 µmol h^{-1} g^{-1}	14
CuBDC-FBA	5 mg catalyst in aqueous TEOA (10%), EY, 300 Xe lamp with UV filter	16829 µmol h^{-1} g^{-1}	15
Cu-RSH coordination polymer	5 mg catalyst in 15 mL 10% aqueous TEOA, EY, 300 W Xe lamp with UV filter	7880 µmol h^{-1} g^{-1}	16

References

1. Z. Jin, H. Yang. *Nanoscale. Res. Lett*., 2017, **12**, 539.
2. S. Dash, S. Prakash Tripathy, S. Subudhi, L. Acharya, A. Ray, P. Behera, K. Parida. *Energy Adv*., 2024, **3**, 1073-1086.
3. J. Cai, B. Liu, S. Zhang, L. Wang, Z. Wu, J. Zhang, B. Cheng. *J. Mater. Sci. Technol*., 2024, **197**, 183-193.
4. S. Prakash Tripathy, S. Subudhi, S. Das, M. Kumar Ghosh M. Das, R. Acharya, R. Acharya, K. Parida. *J. Colloid Interface Sci*., 2022, **606**, 353-366.
5. S. Wang, Z. Ai, X. Niu, W. Yang, R. Kang, Z. Lin, A. Waseem, L. Jiao, H.-L. Jiang. *Adv. Mater*., 2023, 2302512.
6. B. Liu, J. Cai, J. Zhang, H. Tan, B. Cheng, J. Xu. Chin. *J. Catal*., 2023, **51**, 204-215.
7. H. Chang, Y. Li, X. Jia, Q. Shen, Q. Li, X. Liu, J. Xue. *Mater.Sci. Semicon. Proc*., 2022, **150**, 106914.
8. B. Liu, K. Meng, B. Cheng, L. Wang, G. Liang, C. Bie. *J. Mater. Sci. Technol*., 2025, **231**, 286-295.
9. S. Kampouri, F.M. Ebrahim, M. Fumanal, M. Nord, P.A. Schouwink, R. Elzein, R. Addou, G.S. Herman, B. Smit, C.P. Ireland, K.C. Stylianou. *ACS Appl. Mater. Interfaces,* 2021, **13**, 14239-14247.
10. M. Humayun, M. He, W. Feng, C. Jin, Z. Yao, Y. Wang, W. Pi, S. Ali, A. Khan, M. Wang, Z. Zheng, Q. Fu, H. Xia, W. Luo. *Solar Energy,* 2021, **215**, 121-130.
11. R. Abazari, S. Sanati, N. Li, J. Qian. *Inorg. Chem*., 2023, **62**, 18680-18688.
12. P. Zhu, C. Feng, Q. Liang, M. Zhou, Z. Li, S. Xu. *Ceram. Int*., 2023, **49**, 20706-20714.
13. J. Zhao, Y. Wang, J. Zhou, P.Qi, S. Li, K. Zhang, X. Feng, B. Wang, C. Hu. *J. Mater. Chem. A,* 2016, **4**, 7174-7177.
14. S. Panda, R. Bariki, S. Kumar Pradhan, S. Kumar Nayak, B. Gopal Mishra. *ACS Appl. Nano Mater*., 2024, **7**, 7365-7380.
15. C. Guo, T. Wang, L. Zhang, T. Chen, C. Guo, A. Hassan, N. Akram, Y. Kou, J. Wang. *Nanoscale,* 2022, **14**, 15316-15326.
16. X.Y. Dong, M. Zhang, R.-B. Pei, Q. Wang, D.-H. Wei, S.-Q. Zang, Y.-T. Fan, T.C.W. Mak. *Angew. Chem. Int. Ed*., 2016, **55**, 2073-2077.